Thermal and photocatalytic stability enhancement mechanism of poly(propylene carbonate) due to Cu(I) impurities

Erdal Uzunlar, Paul A. Kohl*

School of Chemical and Biomolecular Engineering, Georgia Institute of Technology, Atlanta, GA 30332-0100, USA

ABSTRACT

The thermal and photolytic decomposition of poly(propylene carbonate) (PPC) in the presence of a photoacid generator (PAG) was studied. The mechanism of previously observed shifts in the decomposition temperature of PPC was investigated. The decomposition temperature of PPC can be altered when PPC/PAG films contact copper metal. X-ray photoelectron spectroscopy (XPS) analysis showed that a small amount Cu(I) was incorporated into the PPC/PAG film causing the increased stability and the Cu(I) concentration was similar to that of the PAG. PPC/PAG temperature stability was studied for a number of iodonium and sulfonium-based PAGs. Every iodonium-based PAG showed a PPC decomposition temperature shift and no sulfonium-based PAG showed the thermal stability effect. It appears that Cu(I) interacts with iodonium in the cation of the PAG causing a change in the acid creation mechanism of the PAG.

© 2012 Elsevier Ltd. All rights reserved.

1. Introduction

Sacrificial polymers have been used in the microfabrication of a variety of microelectromechanical (MEMS) and microfluidic devices. The basic function of the sacrificial polymer is to provide a space holder for micro-cavity creation [1,2]. Recently, sacrificial polymers have been used to fabricate air-gaps as an ultra low-k insulator for electronic devices and packages [2—11]. Air-clad electrical connections provide a low-loss transmission media for electrical signals, particularly at high frequencies where both the real and imaginary parts of the dielectric constant are important [4—6]. The decomposition temperature of the sacrificial polymer is critically important in the process sequence since it must be compatible with the substrate, encapsulating material(s), and subsequent processing steps [12]. The selection of materials and methods of fabrication are thus limited by the chosen sacrificial polymer. For that reason, there is a clear need to control or fine-tune the decomposition temperature of the sacrificial polymer to accommodate a wide range of materials and processes.

Polynorbornenes [2,7,13—16] and polycarbonates [5,16—22] have been widely used as sacrificial polymers. Polycarbonates generally have a lower decomposition temperature than polynorbornenes and can be used with a wide variety of permanent dielectrics, however, their low glass transition temperature (T_g) can lead to mechanical problems during fabrication. The decomposition of polycarbonates has been catalysed by photoacid generators (PAGs) making them photopatternable [12]. Poly(propylene carbonate) (PPC) can be obtained by the copolymerization of carbon dioxide and propylene oxide using organometallic catalysts [23]. PPC has a modest decomposition temperature, ranging from 100 °C to 300 °C depending on its molecular weight. There are two mechanisms for PPC decomposition: (i) chain unzipping from the end group, and (ii) random chain scission [24—29]. Chain unzipping reaction occurs at lower temperatures compared to chain session because it has a lower activation energy compared to chain scission [24—26,28,29]. In most studies, chain unzipping is shown to be the primary decomposition mechanism [24—26,28,30,31]. It is postulated that chain unzipping occurs either by (i) alkoxide activation where a relatively strong nucleophile at the chain end attacks the carbonyl atom, or (ii) carbonate activation where a relatively weak electrophile attacks the electrophilic carbon atom [29,30,32]. It is also proposed that when the temperature is ramped from low to high, the PPC decomposition takes place in three stages: (i) at lower temperature, chain unzipping is the primary degradation mechanism, (ii) at modest temperatures, decomposition takes place by competing multi-step reactions, and (iii) at the higher temperatures, chain scission dominates the decomposition [33].

There are numerous studies in the literature focussing on increasing the thermal stability of PPC through blending with fillers [27,34—42], polymerizing with additional backbone components [43—49], adding cross-linking [50,51], hydrogen-bonding [41,42,52], end-capping [24,26,33,46], and metal ion coordination [21,25]. Among these, end-capping is the most efficient technique. It also provides simple processing and lower cost. Basically, the

* Corresponding author.
E-mail address: kohl@gatech.edu (P.A. Kohl).

nucleophilic hydroxyl groups at the PPC ends are replaced with less reactive groups inhibiting the hydroxyl initiated chain unzipping reaction. Taking the temperature at the point where 5% weight loss occurs as the characteristic temperature for decomposition (i.e. 5 wt% loss point), Dixon et al. reported ca. 20 °C increase in thermal stability (at 2.5 °C/min heating rate) using acetyl chloride/pyridine reagent as the end-capping agent [24]. Peng et al. observed improved thermal stability by 27 °C–42 °C (at 5 wt% loss point using 10 °C/min heating rate) by end-capping PPC with phosphorous oxychloride, acetic anhydride, ethyl silicate, benzoyl chloride, and maleic anhydride reagents [26]. Yao et al. showed a thermal stability increase of ca. 140 °C (at 5 wt% loss using 15 °C/min heating rate) where PPC was end-capped with maleic anhydride with weight fractions between 0.5 wt% and 5 wt% through melt blending [33].

Improving the thermal stability of PPC by metal ion coordination is another technique in which chain unzipping is inhibited through coordination between a metal ion and oxygen in the carbonate groups. Yu et al. showed that the thermal stability of PPC is significantly enhanced with calcium stearate [25]. It was speculated that Ca cations coordinate with oxygen in the carbonate groups throughout the PPC backbone leading to inhibition of the chain unzipping reaction. Recently, Spencer et al. reported ca. 50 °C increase in thermal stability of PPC (at 50 wt% loss point using 0.5 °C/min heating rate) by copper ion incorporation [21]. The substrate was a copper-sputtered silicon wafer where the native oxide on the copper surface was removed before solvent casting the PPC film. The PPC was cast from a solution containing γ-butyrolactone (GBL) as the solvent and Rhodorsil-FABA as the photoacid generator (PAG). Rhodorsil-FABA is an iodonium-based PAG with a borate anion, as shown in Table 1. The PAG can be activated photolytically (i.e. UV radiation) or thermally. Upon activation, the PAG cation produces two radicals which react either with the hydrocarbon portion of the cation, polymer, or residual solvent to create a proton in order to catalyse the decomposition of the PPC [53].

Spencer et al. [21] observed an increase in the thermal stability when the PPC/PAG mixture was coated on copper for both the UV exposed and unexposed cases. As seen in Fig. 1, the samples prepared on copper (cases labelled "Cu exposed" and "Cu unexposed") both decompose at higher temperatures relative to the samples prepared on silicon (cases labelled "Si exposed" and "Si unexposed"). The decomposition temperature of the unexposed film on copper ("Cu unexposed" case) was even higher than the decomposition temperature of neat PPC. Thus, it is clear that observed thermal stability effect is directly related to the presence of the copper surface. Even though copper incorporation is obviously responsible for thermal stability, the cause of the shift in decomposition temperature was only speculated. It was shown that only trace amounts of copper are needed, estimated to be one copper ion per 100 PPC monomer units (or carbonyl oxygens). The authors discussed that the copper may hinder the unzipping reaction by interacting with the PPC chain ends, so that the decomposition of PPC becomes suppressed. However, there is a scarcity of copper available for interaction with polymer. In addition, there may be no specificity of chain ends to interact with copper, i.e. it is not guaranteed that the copper will interact with PPC chain end rather than with the backbone. The specificity of the interaction between copper and PPC chain end was not discussed in [21].

In this work, the details of the change in thermal stability with contact to copper have been investigated. It is proposed that rather than the copper ions interacting with PPC, a copper-PAG interaction occurs. X-ray photoelectron spectroscopy (XPS) was used to identify the oxidation state of the dissolved copper as Cu(I). A general mechanism for thermal stability is proposed in which copper ion

interacts with iodonium moiety of the Rhodorsil-FABA PAG forming a Cu(I)-I complex so as to inhibit acid creation, thus leading to the apparent increase in the stability of the PPC. The mechanism and interaction with the iodonium-based PAG were tested by examining the thermal decomposition of PPC films with three iodonium-based PAGs and two sulfonium-based PAGs.

2. Experimental

PPC with a molecular weight of 179,000 g/mol was obtained from Novomer Inc. The decomposition temperature (at 50% weight loss) was 210 °C as determined by thermogravimetric analysis (TGA) using 0.5 °C/min heating rate. PPC was used as-received without purification. The PPC/PAG solutions were prepared by mixing PPC with the PAG in γ-butyrolactone (GBL) solvent. The PAGs used in this study were either iodonium-based PAGs including 4-methylphenyl[4-(1-methylethyl)phenyl]iodonium tetrakis(pentafluorophenyl)borate (Rhodorsil-FABA), bis(4-tert-butylphenyl)iodonium triflate (BTBPI-TF), bis(4-tert-butylphenyl)iodonium perfluoro-1-butanesulfonate (BTBPI-NF) and diphenyliodonium triflate (DPI-TF), or sulfonium-based PAGs including tris[4-(4-acetylphenyl)sulfanylphenyl]sulfonium tetrakis(pentafluorophenyl)borate (Irgacure PAG 290, TAPSPS-FABA in this study) and tris[4-(4-acetylphenyl)sulfanylphenyl]sulfonium tris(trifluoromethylsulfonyl)methide (Irgacure GSID 26-1, TAPSPS-TMM in this study). The chemical structures and suppliers of PAGs are shown in Table 1. The PAGs were used as-received. It is assumed that each PAG could produce one proton upon activation. Each PPC/PAG solution was prepared to have the same PAG molar concentration. A 3 wt% Rhodorsil-FABA PAG, with respect to PPC, was taken as the standard concentration so that a direct comparison could be made to previous studies [21]. The required amounts of PAGs as a weight percentage of PPC were calculated accordingly. The molecular weights and required amounts of PAGs in the PPC/PAG solutions are listed in Table 2. Amount of GBL added was four times the amount of PPC, so that the PPC/PAG solutions were each 20 wt% PPC in GBL. For UV–vis spectroscopy experiments, a solution of 20 wt% PPC in GBL without Rhodorsil-FABA was prepared.

Silicon wafers with <100> orientation were supplied from University Wafers. The polymer films were spin coated using a CEE spinner onto either bare silicon wafers with a native oxide (no prior oxide cleaning) or wafers sputtered with Ti/Cu (300 Å/3000 Å) using a Unifilm DC sputterer. The Ti/Cu sputtered wafers were cleaned in a 11 vol% H_2SO_4 in de-ionized (DI) water solution for 30 s with agitation before use in order to remove the native oxide on the copper. After the acid dip, the wafers were rinsed with DI water and dried with N_2. All polymer films were spin-coated to a thickness of ca. 10 μm using a spin speed of 1000 rpm for 40 s. The samples were then soft-baked at 105 °C for 5 min on a hot plate. An Oriel Instruments Hg(Xe) lamp with 248 nm optics was used to irradiate the "exposed" samples to UV radiation at a dose of 154 mW/cm^2 per μm of film thickness. No post-exposure baking was performed on the samples except the ones prepared for X-ray photoelectron spectroscopy (XPS) analysis.

XPS analyses were performed to investigate the oxidation state of the copper in the polymer films. The XPS sample was a Ti/Cu sputtered silicon wafer with a 11 μm thick, UV-irradiated PPC film containing Rhodorsil-FABA PAG. The sample was post-exposure baked at 105 °C for 5 min in order to obtain a copper-rich layer which was identified as responsible for the shift in decomposition temperature, as described previously [21]. After the post-exposure bake, the thickness of the polymer was measured as 6.4 μm, a value which is consistent over a range of experiments. Thus, it was concluded that copper ions migrate into the first ca. 7 μm of the film and cause the shift in decomposition temperature. A Thermo K-

Table 1
The trade names, suppliers and chemical structures of PAGs.

Trade name	Supplier	Chemical structure
Rhodorsil-FABA	Rhodia	
BTBPI-TF	Sigma–Aldrich	
BTBPI-NF	Sigma–Aldrich	
DPI-TF	Sigma–Aldrich	
Irgacure PAG 290 (TAPSPS-FABA in this study)	Ciba/BASF	
Irgacure GSID 26-1 (TAPSPS-TMM in this study)	Ciba/BASF	

Alpha XPS tool was used for XPS analysis on the surface of copper-rich PPC layer. The binding energies for copper species were scanned between 925 eV and 965 eV with a step size of 0.1 eV. The elements present on the surface of the sample were scanned in elemental survey mode between −10 eV and 1350 eV with a 1 eV step size.

TGA experiments were performed to characterize the decomposition temperature of the polymer samples. Small pieces of
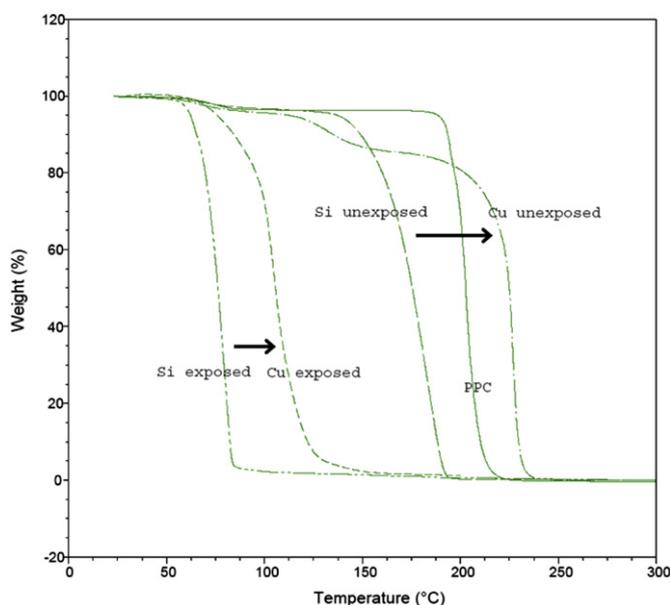
Fig. 1. Dynamic TGA plots for PPC films in GBL cast on a copper surface and cast on silicon with and without UV exposure compared with decomposition of neat PPC without UV exposure.

polymer film were removed from the silicon substrates using a clean razor blade and loaded into platinum TGA pans. A Q50 dynamic thermogravimetric analyser from TA Instruments was used. The temperature ramp rate was 0.5 °C/min for the TGA runs. The decomposition chamber was purged with nitrogen at a flow rate of 40 ml/min at the balance and 60 ml/min at the sample. The microbalance was zeroed prior to each TGA run.

UV−vis spectroscopy analysis was performed in order to evaluate the absorbance of the polymer solutions. UV−vis spectra were measured using Agilent 8453 UV−vis spectrophotometer and Quartz cuvettes (283 QS 1.000). Using a GBL blank, six samples were investigated: No PAG, Mixture, Cu Exposed, Si Exposed, Cu Unexposed, and Si Unexposed. The copper-sputtered or bare silicon substrates were spin-coated with PPC/Rhodorsil-FABA PAG solution, soft-baked, and exposed, if necessary. Pieces of polymer film were removed from the substrates, weighed, loaded into vials and diluted with fresh GBL to make the PAG concentration 0.286 μmol/ml. The amount of GBL required for dilution was calculated assuming that all GBL in the PPC film evaporated during soft-bake. This assumption was adequate for mixture calculations, however, Spencer et al. showed that a small amount of residual solvent remained in the films after soft-bake, which may affect the onset temperature of the decomposition [30]. All samples, except the ones identified as "No PAG" and "Mixture", were transferred into the cuvettes and the UV−vis spectra were measured. The "Mixture" sample was prepared by diluting the Rhodorsil-FABA solution directly with a certain amount of GBL in a vial in order

Table 2
The molecular weights (g/mol) and required amounts of PAGs in the solutions expressed as wt% of PPC.

PAG	Molecular weight (g/mol)	Required wt% of PPC
Rhodorsil-FABA	1016.25	3.00
BTBPI–TF	542.39	1.60
BTBPI–NF	692.42	2.04
DPI–TF	430.18	1.27
TAPSPS–FABA	1393.01	4.11
TAPSPS–TMM	1125.19	3.32

to make the PAG concentration 0.286 μmol/ml, without spin-coating the solution on a substrate and collecting the baked film. In order to prepare the "No PAG" sample, a 20 wt% PPC in GBL solution with no Rhodorsil-FABA PAG was put into a vial and diluted with GBL whose amount was calculated assuming the PPC solution contained PAG. Since the UV−vis spectroscopy samples were prepared to have the same concentrations, the UV−vis spectroscopy results would enable us to assign the absorbance peaks and wavelengths to certain species and assess the changes in their concentrations through changes in corresponding absorbance values.

3. Results

It was previously shown that the oxidation and dissolution of trace amounts of copper in the PPC is essential for observed thermal stability increase [21]. However, the oxidation state of the dissolved copper, which is important in determining the role of copper, was not identified. XPS analysis was used here to determine the oxidation state of the copper in the PPC film after the copper was incorporated into it.

An experiment was done in order to understand the copper oxidation event. A small amount of copper nano-powder was added to the PPC/Rhodorsil-FABA PAG solution. The solution was mixed by ball-milling for two days and then left for 3 weeks. The solution colour turned from colourless to turquoise after 3 weeks indicating the presence of copper ions. The most probable oxidizing agent in the PPC/PAG solution is dissolved oxygen from air. Even if there were a small amount of PAG decomposition over time creating an acid, hydrogen ions do not have a suitable redox potential for copper oxidation, unless a ligand is present for copper complexation.

The sample used for XPS analysis was prepared by spin-coating a copper surface with a PPC/Rhodorsil-FABA PAG solution, and allowing the copper to oxidize and dissolve into the PPC, as explained in the Experimental section. The XPS spectra obtained from the surface of the sample are shown in Fig. 2. The full XPS scan in Fig. 2a shows the presence of Cu, F, O, and C, as expected. The intensity of the Cu peak is very small since there are only trace amounts present in the PPC film. The atomic and mass percentages of the elements in Fig. 2a are shown in Table 3. There was no iodine identified because of its low concentration in the mixture. One can see from the relative intensity of the fluorine peak that iodine would have a very low intensity peak because the atomic ratio of I to F is 1:20 (see PAG structure in Table 1). The peak binding energies in the Cu scan are 933.18 eV and 952.88 eV, as shown in Fig. 2b, corresponding to Cu(I) [54−59]. No Cu(II) peaks were identified. Cu(I) is stable in the presence of an oxidizing agent like oxygen only when it is complexed because it is easier to oxidize Cu(I) to Cu(II) than it is to oxidize Cu(0) to Cu(I). Thus, once Cu(0) is oxidized to Cu(I), it is immediately oxidized to Cu(II), unless Cu(I) is stabilized by a complexing agent. The presence of an iodide-containing species in the mixture was considered as a possible source of a suitable complexing agent for Cu(I) [60]. There are no other obvious choices of ligands for stabilizing Cu(I) in the mixtures used in this study. It is also noted that the concentration of Cu(I) in the film observed previously is about the same as that of the iodonium-based PAG in the mixture [21]. Thus, we conclude that the most likely form of copper dissolved in the PPC/PAG mixture is a Cu(I)-I complex. If this hypothesis were true, then the thermal stability effect of the PPC on a copper surface would be specific to an iodonium-based PAG, and it would not be observed with other PAGs (non-iodonium ones) or other acids.

To test the iodonium-specific copper/PAG interaction, mixtures with sulfonium-based PAGs were investigated. Sulfonium-based
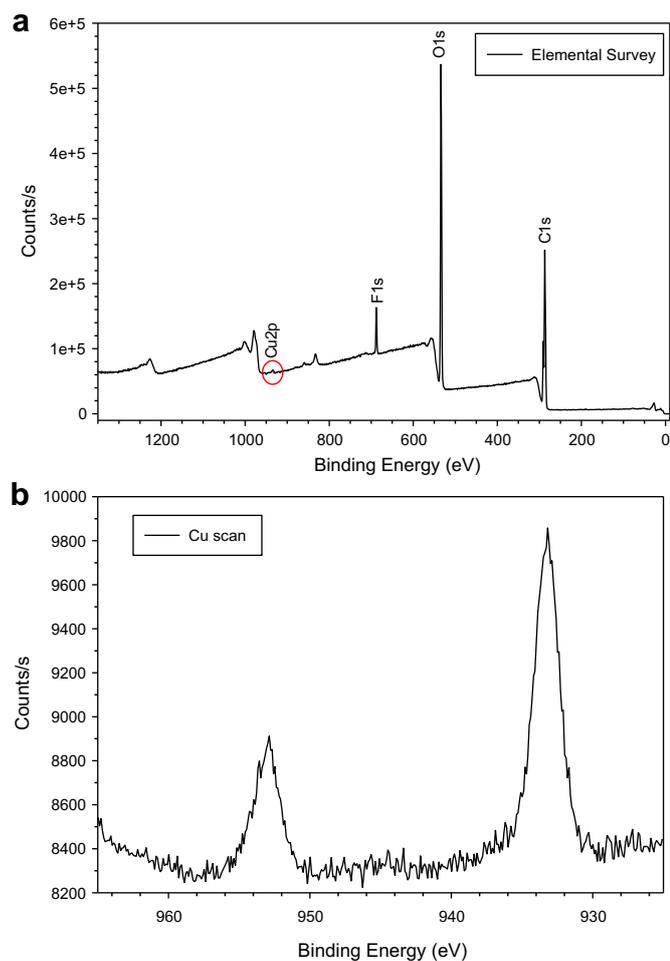
Fig. 2. XPS scans on surface of a PPC film cast on copper surface, UV exposed and post-baked a) Elemental survey b) Cu scan.

Fig. 3. TGA results for PPC films containing sulfonium-based PAGs a) TAPSPS-FABA b) TAPSPS-TMM.

PAGs also produce a strong acid, which can be used to catalytically decompose polycarbonates [53]. Two sulfonium-based PAGs, TAPSPS-FABA and TAPSPS-TMM, whose structures are shown in Table 1, were investigated in the decomposition experiments. The two sulfonium-based PAGs have the same cations with different anions. Since the strength of the acid is related to conjugate base formed (i.e. the anion part of the PAG), the effect of a different anion was investigated. In addition, the anion in TAPSPS-FABA is the same as that in Rhodorsil-FABA. This allows a direct comparison of the cation effect. The sulfonium-based PAGs have a higher molecular weight than Rhodorsil-FABA. The mass loading of the sulfonium-based PAGs in the PPC/PAG solutions were adjusted so as to maintain the same PAG-to-PPC mole ratio as used in the Rhodorsil-FABA solutions.

The TGA results for the PPC films containing sulfonium-based PAGs are shown in Fig. 3. The set of TGA results follows a consistent pattern and they are discussed together. The sample which

Table 3
XPS analysis results for elements and relative percentages.

Element	Atomic percent	Weight percent
Cu	0.06	0.28
F	3.62	4.99
O	37.43	43.45
C	58.86	51.29

was prepared by solvent casting the PPC/sulfonium-based PAG solution onto copper-sputtered substrate followed by UV exposure was labelled "Cu Exposed". A similar sample was prepared but on a silicon substrate and labelled "Si Exposed". UV irradiation of the PAG creates an acid which catalyses the decomposition of PPC lowering the decomposition temperature for the PPC. The decomposition of neat PPC, labelled "PPC", is also shown in Fig. 3. 50% weight loss temperature was taken as the characteristic temperature for decomposition. The value for the UV-exposed samples on copper and silicon was about 100 °C. It is important to note that there is almost no difference in the decomposition profiles for the Si Exposed and Cu Exposed samples here, contrary to the case of the iodonium-based PAG solution. If the cause of the temperature shift on the copper surface was an acid-only effect, then the TGA results with sulfonium-based PAGs would be similar to those of the iodonium-based PAGs. On the other hand, if the interaction of the copper is with the iodide in the PAG, the presence of Cu(I) in the PPC/sulfonium-based PAG film would have no impact on thermal stability, which it doesn't as shown in Fig. 3.

The samples prepared by solvent casting PPC/sulfonium-based PAG solutions onto copper-sputtered or silicon substrates without UV irradiation are labelled "Cu Unexposed" and "Si Unexposed" in Fig. 3, respectively. In the absence of UV-exposure, PAG thermally decomposes to produce an acid which catalyses the decomposition of PPC. In other words, the decomposition temperature of the PPC

films in the unexposed cases is dictated by the PAG decomposition temperature, as shown previously by Spencer et al. [21]. In Fig. 3, it is seen that the unexposed samples decomposed around 210 °C, except for the initial lower decomposition temperature observed in the Si Unexposed case for TAPSPS-TMM. Since neat PPC also decomposed at 210 °C, it is concluded that PAG decomposition does initiate the PPC decomposition at the lower decomposition temperatures of the TGA scan. More importantly, there is almost no difference in decomposition temperature between the Cu Unexposed and Si Unexposed cases, supporting the hypothesis that the iodide in the iodonium-based PAGs is the species that interacts with Cu(I) leading to thermal stability improvement for PPC.

The set of sulfonium-based PAGs show that copper has virtually no effect on the PPC decomposition temperature. There were small increases in decomposition temperature observed for some of the cases. For example, for TAPSPS-FABA, there was about 5 °C increase in both copper and silicon unexposed cases relative to neat PPC and a 3 °C increase in the Cu Exposed case relative to Si Exposed case. For TAPSPS-TMM, there were 5 °C and 8 °C increases in the copper and silicon unexposed cases relative to neat PPC. There was also a 6 °C increase in Cu Exposed case relative to the Si Exposed case. These increases are small and can be caused by a variety of experimental conditions in the TGA, such as sample contact with the TGA pan. These temperature shifts are insignificant compared to the increases observed by Spencer et al. for the iodonium-based PAG [21]. For that reason, it is reasonable to conclude that there is no significant thermal stability increase observed due to a copper interaction in the exposed and unexposed cases for the sulfonium-based PAGs. Moreover, since the anions of the Rhodorsil-FABA and TAPSPS-FABA are the same, another conclusion is that the thermal stability increase due to copper is directly related to the cation portion of the PAG and not the anion. This supports the idea that iodide is an essential component in the copper-induced suppression of the decomposition in the PPC/PAG films.

In order to confirm that copper-induced PPC decomposition is specific to the iodonium-based PAGs, three iodonium-based PAGs, BTBPI-TF, BTBPI-NF and DPI-TF, whose structures are shown in Table 1, were used in the PPC decomposition experiments. BTBPI-TF and BTBPI-NF have the same cation, whereas BTBPI-TF and DPI-TF have the same anion. In addition, the cation portion of BTBPI-TF and DPI-TF closely resembles the cation portion in Rhodorsil-FABA, where the isopropyl and methyl groups in Rhodorsil-FABA are replaced by tertiary butyl groups in BTBPI-TF and DPI-TF. These similarities allow us to study the effects of both cations and anions on the copper-induced temperature shift for the iodonium-based PAGs. The molecular weights of the iodonium-based PAGs are smaller than Rhodorsil-FABA. The mass loading of the iodonium-based PAGs in the PPC/PAG solutions were adjusted so as to maintain a constant PAG to PPC mole ratio, just as used in the Rhodorsil-FABA solutions. The TGA results for the iodonium-based PAGs are shown in Fig. 4. The TGA results are discussed separately for each iodonium-based PAG.

Fig. 4a shows the TGA results for the solution containing BTBPI-TF PAG. Si Exposed sample decomposed at 101 °C due to UV activation of the PAG and subsequent acid creation. On the other hand, the Cu Exposed sample decomposed at 164 °C, where there was a 63 °C temperature shift relative to the Si Exposed case. This temperature shift due to the presence of copper was consistent with the hypothesis that if there is an interaction between the iodonium portion of the PAG and the dissolved Cu(I) in PPC, the Cu(I) ion appears to inhibit the PAG's ability to create an acid to catalyse PPC decomposition.

For the unexposed cases using BTBPI-TF, there was no thermal stability effect observed, contrary to the Rhodorsil-FABA case. That
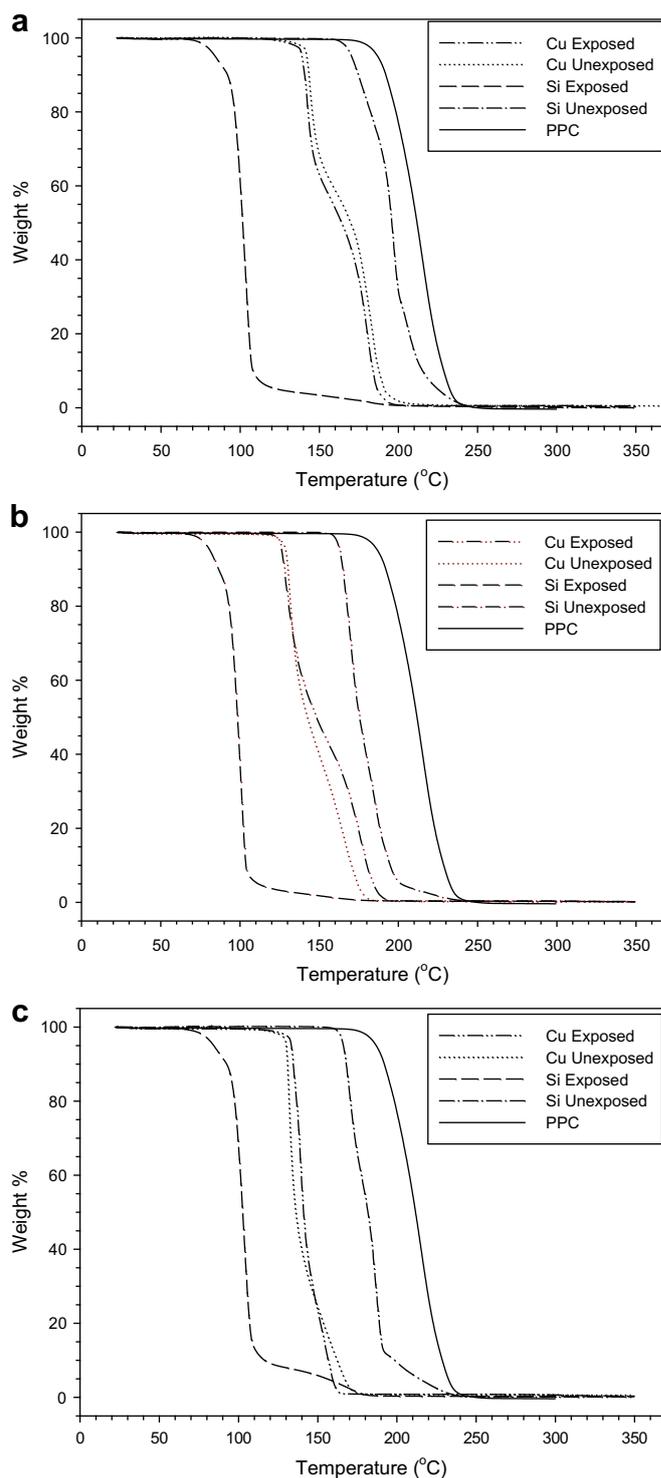

Fig. 4. TGA results for PPC films containing iodonium-based PAGs a) BTBPI-TF b) BTBPI-NF c) DPI-TF.

is, the decomposition temperature of Cu Unexposed sample was not higher than that of the Si Unexposed sample using BTBPI-TF. Contrarily, the Si Unexposed sample decomposed at a higher temperature (196 °C) compared to Cu Unexposed sample (169 °C). In the Si Unexposed case, the thermal activation of the PAG and subsequent acid creation take place lowering the decomposition temperature compared to neat PPC. The situation is, however, more

complex for the Cu Unexposed case. It appears that in the unexposed case, the Cu(I) ion interaction with the PAG destabilizes the PAG and facilitates acid creation, lowering the decomposition temperature relative to both the Si Unexposed case and neat PPC. In contrast to our result, Spencer et al. showed that the decomposition temperature of the Cu Unexposed samples was higher than the Si Unexposed samples. The decomposition temperature was even higher than neat PPC. This observation was left unexplained in the previous study [21]. A combination of the results here with the previous ones in [21] seems to lead to a two-step mechanism for the PPC thermal stability increase. First, Cu(I) inhibits acid creation in the PAG. Second, end-capping of PPC chains occurs by the copper species resulting in a higher thermal decomposition temperature than for neat PPC. This two-step mechanism is plausible because if the Cu(I) inhibits the acid creation, the decomposition temperature of the Cu Unexposed sample should not exceed the neat PPC decomposition temperature. It was previously reported that end-capping increases the thermal stability of PPC [24,26,33,46]. Moreover, there is evidence in the literature for a thermal stability increase facilitated by metal ion coordination with the polymer backbone, as well as chain terminations [21,25]. Thus, in our case, it is possible that the acid creation catalysed in the unexposed case dominated over the end-capping of PPC, so that the net effect observed was the lowering of decomposition temperature for the Cu Unexposed samples. Another interesting result with BTBPI-TF PAG is that the decomposition temperatures of the PPC on copper (exposed or unexposed) were about the same. The values were lower than the value observed for Si Unexposed. This result shows a significant interaction between the Cu(I) and the iodonium cation which results in acid creation independent of UV radiation.

Fig. 4b shows the TGA results for the PPC/BTBPI-NF film. The PPC decomposition behaviour resembles that of BTBPI-TF, shown in Fig. 4a. The Cu Exposed sample decomposed at a higher temperature (148 °C) compared to Si Exposed sample (98 °C), which is consistent with the previous results for the other iodonium-based PAGs. However, no thermal stability was observed for the unexposed cases. That is, the Cu Unexposed sample did not decompose at a higher temperature relative to the Si Unexposed sample due to acid creation, as discussed above. The PAG was thermally activated in the Si Unexposed case and in both cases on copper (exposed and unexposed), as shown by their lower decomposition temperature compared to neat PPC.

The TGA results for the films containing DPI-TF PAG are shown in Fig. 4c. The DPI-TF behaviour is similar to BTBPI-TF and BTBPI-NF. The Cu Exposed sample decomposed at 141 °C whereas the Si Exposed sample decomposed at 103 °C showing the thermal stability increase for the exposed case. As already mentioned, there is no thermal stability increase for the unexposed cases. The decomposition temperatures for the Cu Exposed and Cu Unexposed films for DPI-TF are almost the same as the films containing BTBPI-TF and BTBPI-NF PAGs. This is due to the similarity between the DPI-TF and BTBPI cations.

It appears there are two steps in the TGA plots for PPC decomposition on copper, as shown in Fig. 1 (Cu unexposed case), Fig. 4a, b, and c. Each shows an initial decrease in mass at about 150 °C in the first step followed by further decomposition in the second step at a higher temperature. This appears to be an indication of the complexity of the decomposition mechanism of PPC on copper with some acid being created by the copper-PAG interaction. The decomposition mechanism that occurred at lower temperatures may be different than at higher temperatures, e.g. by chain unzipping in the first region at the lower temperature, and by chain scission in the second region at a higher temperature [24–26,28–30]. There is little or no residue, i.e. less than 0.5 wt%, left after full PPC decomposition which indicates that BTBPI-TF,

BTBPI-NF and DPI-TF PAGs work well with PPC and can be used for air-cavity creation.

In light of the full body of results for the PPC films containing iodonium-based PAGs, it is clear that there is a thermal stability increase for each sample when the film was coated on copper. No iodonium-based PAG was tested that did not show the result. Further, no sulfonium-based PAG showed any temperature effect of copper incorporation. This supports our hypothesis of a Cu(I)-I interaction. A possible explanation for thermal stability increase is that formation of a Cu(I)-I complex disrupts the decomposition of the PAG and its acid creation at the lowest decomposition temperatures (i.e. Cu Exposed). The formation of a Cu(I)-I complex in the unexposed cases seems to lead to two kinds of results. The first is the creation of an acid at a lower temperature than otherwise observed for the PPC/PAG mixture (Fig. 4) and the second is a stabilization of the PPC (Fig. 1).

UV–vis spectroscopy was used to investigate the photo-bleaching of the PAGs and any other effects of UV irradiation. The same Rhodorsil-FABA concentration, 0.286 μmole per ml of GBL solvent, was used in each of the six experiments, corresponding to: No PAG (PPC without PAG), Mixture (PPC and PAG), Cu Exposed, Cu Unexposed, Si Exposed and Si Unexposed. The UV–vis results are shown in Fig. 5 and tabulated in Table 4. The peak observed at 260 nm is due to the absorbance of the PAG and no other peaks were observed in the visible range. There were little changes in peak wavelength or absorbance as a result of UV irradiation or presence of copper. UV irradiation of the PAG and creation of the photoacid did not result in photo-bleaching of the PAG. The peak wavelength likely shifted slightly due to the PAG degradation products, such as toluene and isopropyl benzene, which are very close to each other (261 nm and 258 nm, respectively [61]).

4. Discussion

Since the thermal stability increase of PPC was observed whenever the PPC/Rhodorsil-FABA solution was in contact with the copper surface, a specific interaction between the film and the copper is proposed. The effect was more clearly observed when a fresh copper surface was used where there was no native oxide layer on copper surface before coating the PPC film. This implies that dissolution of the native cupric oxide has no effect on the shift in PPC decomposition temperature. There is convincing evidence in the literature showing that metal ion incorporation can lead to an increase in thermal stability of polymers through the formation of
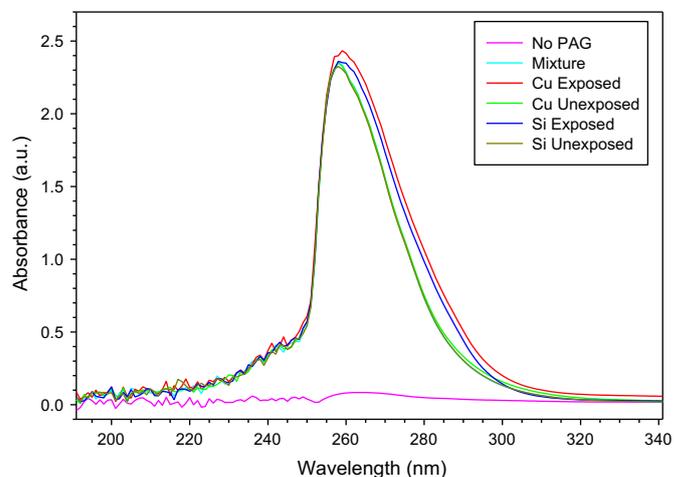

Fig. 5. UV–vis spectroscopy results.

Table 4
UV–vis spectra peak wavelength (nm) and absorbance (AU) values.

Sample	Wavelength (nm)	Absorbance (AU)
No PAG	264	0.084
Mixture	258	2.353
Cu Exposed	260	2.434
Cu Unexposed	258	2.354
Si Exposed	259	2.361
Si Unexposed	258	2.326

complexes with polymer backbones or end-capping of the polymer [21,25,62]. Burrows et al. reported an increase in thermal stability of polyacrylamide by various metal ions such as Cu(II), Fe(II), Ni(II), Hg(I) caused by formation of a metal–polymer complex involving the amide group oxygen [62]. Yu et al. showed the inhibition of the end-initiated, unzipping decomposition of the PPC via Ca(II) coordination with carbonate groups of the PPC chains [25]. In contrast, the copper-initiated results shown here occur with a scarcity of copper ions where there are only 18 copper ions per 1720 monomers monomer units (average polymer chain length) [21]. Moreover, there is no guarantee that copper ions will form complexes with chain ends and not with other sites in the polymer backbone. That is, it is possible for copper ions to interact with the PPC backbone rather than chain ends. Thus, the mechanism of temperature suppression observed here for the Cu(I)/PAG/PPC system is most likely due to a Cu(I)/PAG interaction. The feasible scenario is an interaction between Cu(I) and I in the PAG where a Cu(I)-I complex disrupts the acid creating mechanism of the thermally or photolytically activated PAG. This mechanism is plausible from a stoichiometric point of view since the concentration of copper matches that of the PAG and not that of the PPC or its end groups, according to energy-dispersive x-ray spectroscopy (EDS) analysis in [21]. In addition, it is known that the cation is the portion of PAG responsible for the acid creation and UV absorbance [53]. Moreover, Crivello et al. studied the interaction of copper with diaryliodonium PAGs, such as 4-methyl-phenyl[4-(methylethyl) phenyl] iodoniumtetrakis (pentafluorophenyl)borate (FABA) and showed that Cu(I) is the only ion which interacts with PAGs among a group of ions including Ni(II), Co(II), Fe(II), Ag(I), Mn(III), Cr(III) and Pd(II) [63].

Thus, a mechanism for copper ion complexation with an iodonium-based PAG can be proposed. The Cu(I) ion is formed through oxidation of metallic copper and it forms an iodide complex with the iodide from the PAG, probably degrading the cation of the PAG without acid creation, or stabilizing it to prevent activation and subsequent acid creation. Since the acid is not produced at the same temperature, the thermal stability of PPC increases. Cupric ions have no effect on the PPC decomposition temperature [21].

The copper-PPC interaction proposed by Spencer et al. (i.e. end-capping stabilization) seems unlikely to be the primary effect since the stoichiometry does not match. Further, all iodonium-based PAGs show the temperature shift and no sulfonium-based PAGs give the response even though they may have the same acid strength, as evidenced by the same conjugate base (i.e. common anion experiments). Moreover, it was previously shown that interactions between diaryliodonium salts and a small amount of Cu(I) are essential for the decomposition of diaryliodonium salts [63].

5. Conclusions

The PPC decomposition in the presence of the photolytically or thermally activated PAG was studied. Previously observed shifts in the decomposition temperature of PPC were investigated. The decomposition temperature of PPC can be altered when the PPC/PAG films contact copper metal. XPS results show copper is in the Cu(I) oxidation state. The Cu(I) stoichiometry is similar to that of the PAG. Every iodonium-based PAG shows the PPC temperature shift and no sulfonium-based PAG shows the effect. Thus, it appears that the copper interacts with iodonium in the cation of the PAG and the acid creation mechanism of the PAG changes, often shifting the PPC decomposition to a higher temperature.

References

[1] Peeni BA, Lee ML, Hawkins AR, Woolley AT. Sacrificial layer microfluidic device fabrication methods. Electrophoresis 2006;27:4888–95.
[2] Bhusari D, Reed HA, Wedlake M, Padovani AM, Allen SAB, Kohl PA. Fabrication of air-channel structures for microfluidic, microelectromechanical, and microelectronic applications. Journal of Microelectromechanical Systems 2001;10:400–8.
[3] Kohl P, Zhao Q, Patel K, Schmidt D, Bidstrup-Allen S, Shick R, et al. Air-gaps for electrical interconnections. Electrochemical and Solid State Letters 1998;1:49–51.
[4] Spencer TJ, Osborn T, Kohl PA. Materials science - high-frequency chip connections. Science 2008;320:756–7.
[5] Spencer TJ, Joseph PJ, Kim TH, Swaminathan M, Kohl PA. Air-gap transmission lines on organic substrates for low-loss interconnects. IEEE Transactions on Microwave Theory and Techniques 2007;55:1919–25.
[6] Spencer TJ, Chen JK, Saha R, Bashirullah R, Kohl PA. IEEE. Air cavity low-loss signal lines on BT substrates for high frequency chip-to-chip communication, vols. 1–4; 2009. 2009 IEEE 59th electronic components and technology conference. p. 1221–6.
[7] Park S, Allen SAB, Kohl PA. Air-gaps for high-performance on-chip interconnect part II: modeling, fabrication, and characterization. Journal of Electronic Materials 2008;37:1534–46.
[8] Lee YC, Park CS. A novel CPW-to-stripline vertical via transition using a stagger via structure and embedded air cavities for V-band LTCC SiP applications. Asia-Pacific microwave conference. Suzhou, PR China: IEEE; 2005. p. 1307–10.
[9] Yook JM, Kim KM, Kwon YS. Air-cavity transmission lines on anodized aluminum for high-performance RF modules. IEEE Microwave and Wireless Component Letters 2009;19:623–5.
[10] Song SS, Seo KS. A W-band air-cavity filter integrated on a thin-film substrate. IEEE Microwave and Wireless Component Letters 2009;19:200–2.
[11] Song S, Yoo CS, Seo KS. W-band bandpass filter using micromachined air-cavity resonator with current probes. IEEE Microwave and Wireless Component Letters 2010;20:205–7.
[12] Kelleher H. Georgia tech; 2004. p. 4, 25, 94, 212–6.
[13] Devlin NR, Brown DK, Kohl PA. Patterning decomposable polynorbornene with electron beam lithography to create nanochannels. Journal of Vaccum Science and Technology B 2009;27:2508–11.
[14] Wu XQ, Reed HA, Wang Y, Rhodes LF, Elce E, Ravikiran R, et al. Fabrication of microchannels using polynorbornene photosensitive sacrificial materials. Journal of Electrochemical Society 2003;150:H205–13.
[15] Li WL, Tegenfeldt JO, Chen L, Austin RH, Chou SY, Kohl PA, et al. Sacrificial polymers for nanofluidic channels in biological applications. Nanotechnology 2003;14:578–83.
[16] Joseph PJ, Kelleher HA, Allen SAB, Kohl PA. Improved fabrication of micro air-channels by incorporation of a structural barrier. Journal of Micromechanics and Microengineering 2005;15:35–42.
[17] Reed HA, White CE, Rao V, Allen SAB, Henderson CL, Kohl PA. Fabrication of microchannels using polycarbonates as sacrificial materials. Journal of Micromechanics and Microengineering 2001;11:733–7.
[18] Jayachandran JP, Reed HA, Zhen HS, Rhodes LF, Henderson CL, Allen SAB, et al. Air-channel fabrication for microelectromechanical systems via sacrificial photosensitive polycarbonates. Journal of Microelectromechanical Systems 2003;12:147–59.
[19] White CE, Henderson CL. Photosensitive copolycarbonates for use as sacrificial materials in the fabrication of microfluidic and microelectromechanical devices. Conference on advances in resist technology and processing XXI. Santa Clara, CA: Spie-Int Soc Optical Engineering; 2004. p. 850–60.
[20] Joseph PJ, Monajemi P, Ayazi F, Kohl PA. Wafer-level packaging of micro-mechanical resonators. IEEE Transactions on Advanced Packaging 2007;30:19–26.
[21] Spencer T, Chen Y, Saha R, Kohl P. Stabilization of the thermal decomposition of poly(propylene carbonate) through copper ion incorporation and use in self-patterning. Journal of Electronic Materials 2011;40:1350–63.

[22] Rajarathinam V, Fritz N, Allen SAB, Kohl PA. Imprint lithography enabling ultra-low loss coaxial interconnects. Microelectronic Engineering 2011;88: 240–6.

[23] Inoue S, Koinuma H, Tsuruta T. Copolymerization of carbon dioxide and epoxide. Journal of Polymer Science Part B-Polymer Letters 1969;7:287.

[24] Dixon DD, Ford ME, Mantell GJ. Thermal stabilization of poly(alkylene carbonate)s. Journal of Polymer Science Part C-Polymer Letters 1980;18: 131–4.

[25] Yu T, Zhou Y, Liu K, Zhao Y, Chen E, Wang F, et al. Improving thermal stability of biodegradable aliphatic polycarbonate by metal ion coordination. Polymer Degradation and Stability 2009;94:253–8.

[26] Peng SW, An YX, Chen C, Fei B, Zhuang YG, Dong LS. Thermal degradation kinetics of uncapped and end-capped poly(propylene carbonate). Polymer Degradation and Stability 2003;80:141–7.

[27] Li X, Meng Y, Zhu Q, Tjong S. Thermal decomposition characteristics of poly(propylene carbonate) using TG/IR and Py-GC/MS techniques. Polymer Degradation and Stability 2003;81:157–65.

[28] Liu BY, Zhao XJ, Wang XH, Wang FS. Thermal degradation kinetics of poly(propylene carbonate) obtained from the copolymerization of carbon dioxide and propylene oxide. Journal of Applied Polymer Science 2003;90: 947–53.

[29] Luinstra G. Poly(propylene carbonate), old copolymers of propylene oxide and carbon dioxide with new interests: catalysis and material properties. Polymer Reviews 2008;48:192–219.

[30] Spencer T, Kohl P. Decomposition of poly(propylene carbonate) with UV sensitive iodonium salts. Polymer Degradation and Stability 2011;96: 686–702.

[31] Yan H, Cannon W, Shanefield D. Thermal decomposition behaviour of poly(-propylene carbonate). Ceramics International 1998;24:433–9.

[32] Luinstra G, Haas G, Molnar F, Bernhart V, Eberhardt R, Rieger B. On the formation of aliphatic polycarbonates from epoxides with chromium(III) and aluminum(III) metal-salen complexes. Chemistry-A European Journal 2005; 11:6298–314.

[33] Yao MJ, Mai F, Deng H, Ning NY, Wang K, Fu QA. Improved thermal stability and mechanical properties of poly(propylene carbonate) by reactive blending with maleic anhydride. Journal of Applied Polymer Science 2011;120: 3565–73.

[34] Jiao J, Xiao M, Shu D, Li L, Meng YZ. Preparation and characterization of biodegradable foams from calcium carbonate reinforced poly(propylene carbonate) composites. Journal of Applied Polymer Science 2006;102: 5240–7.

[35] Ma XF, Chang PR, Yu JG, Wang N. Preparation and properties of biodegradable poly(propylene carbonate)/thermoplastic dried starch composites. Carbohydrate Polymers 2008;71:229–34.

[36] Joshi SS, Mebel AM. Computational modeling of biodegradable blends of starch amylose and poly-propylene carbonate. Polymer 2007;48:3893–901.

[37] Zhang ZH, Mo ZS, Zhang HF, Zhang Y, Na TH, An YX, et al. Miscibility and hydrogen-bonding interactions in blends of carbon dioxide/epoxy propane copolymer with poly (p-vinylphenol). Journal of Polymer Science Part B-Polymer Physics 2002;40:1957–64.

[38] Shi XD, Gan ZH. Preparation and characterization of poly(propylene arbonate)/montmorillonite nanocomposites by solution intercalation. European Polymer Journal 2007;43:4852–8.

[39] Wang N, Zhang XX, Yu JG, Fang JM. Partially miscible poly(lactic acid)-blend-poly(propylene carbonate) filled with carbon black as conductive polymer composite. Polymer International 2008;57:1027–35.

[40] Yang DZ, Hu P. Miscibility, crystallization, and mechanical properties of poly(3-hydroxybutyrate) and poly(propylene carbonate) biodegradable blends. Journal of Applied Polymer Science 2008;109:1635–42.

[41] Zhang Z, Shi Q, Peng J, Song JB, Chen QY, Yang JL, et al. Partial delamination of the organo-montmorillonite with surfactant containing hydroxyl groups in maleated poly(propylene carbonate). Polymer 2006;47:8548–55.

[42] Zhang Z, Lee JH, Lee SH, Heo SB, Pittman CU. Morphology, thermal stability and rheology of poly(propylene carbonate)/organoclay nanocomposites with different pillaring agents. Polymer 2008;49:2947–56.

[43] Thorat SD, Phillips PJ, Semenov V, Gakh A. Physical properties of aliphatic polycarbonates made from CO2 and epoxides. Journal of Applied Polymer Science 2003;89:1163–76.

[44] Gao LJ, Xiao M, Wang SJ, Du FG, Meng YZ. Covolvmerization of carbon dioxide and provvlene oxide with zinc glutarate in the presence of compounds containing active hydrogen. Journal of Applied Polymer Science 2007;104:15–20.

[45] Gao LJ, Xiao M, Wang SJ, Meng YZ. Thermally stable poly(propylene carbonate) synthesized by copolymerizing with bulky naphthalene containing monomer. Journal of Applied Polymer Science 2008;108:1037–43.

[46] Song PF, Xiao M, Du FG, Wang SJ, Gan LQ, Liu GQ, et al. Synthesis and properties of aliphatic polycarbonates derived from carbon dioxide, propylene oxide and maleic anhydride. Journal of Applied Polymer Science 2008;109: 4121–9.

[47] Lu LB, Huang KL. Synthesis and characteristics of a novel aliphatic polycarbonate, poly (propylene oxide)-co-(carbon dioxide)-co-(gamma-butyrolactone). Polymer International 2005;54:870–4.

[48] Liu QY, Zou YN, Bei YL, Qi GB, Meng YZ. Mechanic properties and thermal degradation kinetics of terpolyrner poly(propylene cyclohexene carbonate)s. Materials Letters 2008;62:3294–6.

[49] Lu LB, Liu SQ, Huang KL. Molecular simulation of structure and loading-drug character of poly(propylene-co-gamma-butyrolactone carbonate). Journal of Applied Polymer Science 2008;107:872–80.

[50] Qin YS, Ma QW, Wang XH, Sun JZ, Zhao XJ, Wang FS. Electron-beam irradiation on poly(propylene carbonate) in the presence of polyfunctional monomers. Polymer Degradation and Stability 2007;92:1942–7.

[51] Tao YH, Wang XH, Zhao XJ, Li J, Wang FS. Crosslinkable poly(propylene carbonate): high-yield synthesis and performance improvement. Journal of Polymer Science Part A-Polymer Chemistry 2006;44:5329–36.

[52] Yu T, Zhou Y, Zhao Y, Liu KP, Chen EQ, Wang DJ, et al. Hydrogen-bonded thermostable liquid crystalline complex formed by biodegradable polymer and amphiphilic molecules. Macromolecules 2008;41:3175–80.

[53] Cupta M, Joseph P, Kohl P. Photoacid generators for catalytic decomposition of polycarbonate. Journal of Applied Polymer Science 2007;105:2655–62.

[54] Chawla SK, Sankarraman N, Payer JH. Diagnostic spectra for xps analysis of cu-o-s-h compounds. J Electron Spectrosc Relat Phenom 1992;61:1–18.

[55] Khattak GD, Mekki A, Al-Shukri A. X-ray photoelectron spectroscopy study of copper tellurite glasses. Physica Scripta 2004;70:187–92.

[56] Yin M, Wu CK, Lou YB, Burda C, Koberstein JT, Zhu YM, et al. Copper oxide nanocrystals. Journal of American Chemical Society 2005;127:9506–11.

[57] Stadnichenko AI, Sorokin AM, Boronin AI. XPS, UPS, and STM studies of nanostructured CuO films. Journal of Structural Chemistry 2008;49:341–7.

[58] Ghodselahi T, Vesaghi MA, Shafiekhani A, Baghizadeh A, Lameii M. XPS study of the Cu@Cu(2)O core-shell nanoparticles. Applied Surface Science 2008;255:2730–4.

[59] Ghijsen J, Tjeng LH, Vanelp J, Eskes H, Westerink J, Sawatzky GA, et al. Electronic-structure of Cu₂O and CuO. Physical Review B 1988;38:11322–30.

[60] Sillen LG. Stability constants of metal-ion complexes. Supplement no. 1. 2nd ed. London: Chemical Society; 1971.

[61] NIST chemistry webbook, http://webbook.nist.gov/chemistry/

[62] Burrows H, Ellis H, Utah S. Adsorbed metal-ions as stabilizers for the thermaldegradation of polyacrylamide. Polymer 1981;22:1740–4.

[63] Crivello J, Lockhart T, Lee J. Diaryliodonium salts as thermal initiators of cationic polymerization. Journal of Polymer Science Part A-Polymer Chemistry 1983;21:97–109.